



ELSEVIER

Contents lists available at SciVerse ScienceDirect

Materials Letters

journal homepage: www.elsevier.com/locate/matlet

Size-controllable hydrothermal synthesis of ZnS nanospheres and the application in photocatalytic degradation of organic dyes

Fangfang Dong, Yuming Guo*, Jie Zhang, Yihui Li, Lin Yang*, Qilong Fang, Hui Fang, Kai Jiang

School of Chemistry and Chemical Engineering, Engineering Technology Research Center of Motive Power and Key Materials of Henan Province, Henan Normal University, Xinxiang 453007, PR China

ARTICLE INFO

Article history:

Received 26 October 2012

Accepted 9 January 2013

Available online 20 January 2013

Keywords:

ZnS nanospheres

Semiconductors

Size-controllable

Functional

Photocatalysis

ABSTRACT

Herein, using histidine as the additive, well-dispersed ZnS nanospheres with the controllable size and large specific surface area were prepared successfully in large scale via a facile one-pot hydrothermal synthesis method. The as-prepared ZnS nanospheres exhibited strong photo absorption in the UV and visible light region. From the results, the as-prepared ZnS nanospheres prepared at 160 °C for 6 h could photocatalytically degrade the rhodamine B efficiently through the mediation of photo-generated hydroxyl radicals under UV light irradiation. These suggest that the ZnS nanospheres prepared in this study might be used as the potential photocatalysts to treat the organic pollutants efficiently.

© 2013 Elsevier B.V. All rights reserved.

1. Introduction

Currently, with the rapid development of textile dyeing industry, extremely large amount of toxic organic pollutants were discharged and lead to serious ecological and environmental issues [1,2]. Therefore, environmental problems related with toxic pollutants provide the major driving force for the research of the environmental management. However, the efficient treatment of these pollutants through facile approaches has remained a great challenge. Photocatalytic treatment displays great potential for elimination of toxic pollutants because of its efficiency and applicability [3,4]. During the past decades, various novel semiconductor catalysts for photocatalysis have been synthesized and studied, in which TiO₂ is generally used as the catalyst in photochemistry and environmental protection [5,6]. Recently, transition-metal sulfides, e.g. ZnS and CdS, have been intensively studied because of their unique advantages compared to TiO₂ [7–10]. As one of the important semiconductors, ZnS has wide band gap energy of 3.5–3.7 eV for cubic zinc blend structure and 3.7–3.8 eV for hexagonal wurtzite structure [11]. Recently, ZnS nanomaterials have been extensively investigated and exhibited important applications in various fields, such as optics, electronics, and photocatalysis [12,13]. However, the practical applications of ZnS nanomaterials in photocatalysis are seriously limited because of the high cost of their large scale production, coupled with the tremendous difficulties in separation and recycling.

Herein, a facile procedure for large-scale production by using a low-cost hydrothermal approach to prepare the well-dispersed ZnS nanospheres with the controllable size and large specific surface area (SSA) was reported. The ZnS nanospheres prepared at 160 °C for 6 h exhibited good photocatalytic activity for degradation of rhodamine B (RhB).

2. Materials and methods

For the typical preparation of the well-dispersed ZnS nanospheres, histidine (C₆H₉N₃O₂) and zinc acetate with 1:1 M ratio were dissolved into double distilled water and incubated for 2 h. Then, thioacetamide aqueous solution was added. Subsequently, the reaction mixture was transferred into a Teflon lined autoclave, sealed and heated at 160 °C for 6 h. Finally, the product was centrifuged, washed, and dried under vacuum at 30 °C. For comparison, the experiments were also performed at 140 °C and 180 °C. The products are denoted as ZnS-140, ZnS-160 and ZnS-180 nanospheres, respectively. In addition, the reaction time was prolonged to 12 and 24 h to determine the effect of the reaction time on the morphology and size of the products.

The size and morphology of the products were analyzed by scanning electron microscopy (SEM). The XRD patterns were recorded on diffractometer with Cu K α radiation source ($\lambda=1.5406 \text{ \AA}$). The UV–vis absorption spectra of the ZnS nanospheres were recorded. The SSA of the ZnS nanospheres were analyzed through the Brunauer–Emmett–Teller (BET) determination using N₂ as an adsorbent.

For photocatalytic activity evaluation, 20 mL of ZnS nanospheres aqueous suspension (1 mg/mL) were mixed with 30 mL of RhB

* Corresponding authors. Tel.: +86 373 3325058; fax: +86 373 3328507.

E-mail addresses: guoyuming@gmail.com (Y. Guo), yanglin1819@163.com (L. Yang).

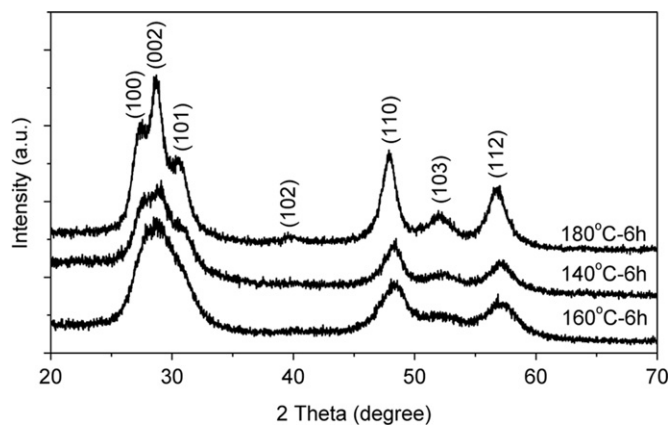


Fig. 1. XRD patterns of ZnS-140, ZnS-160 and ZnS-180 nanospheres.

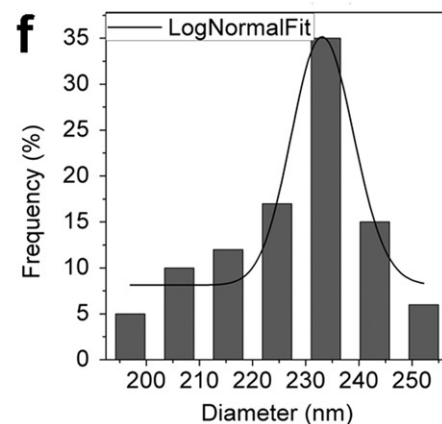
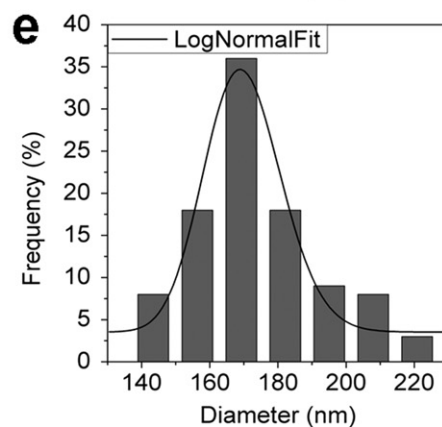
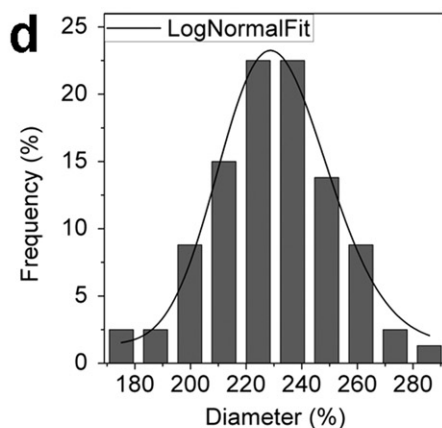
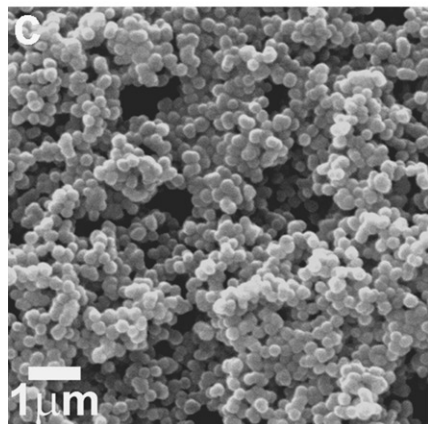
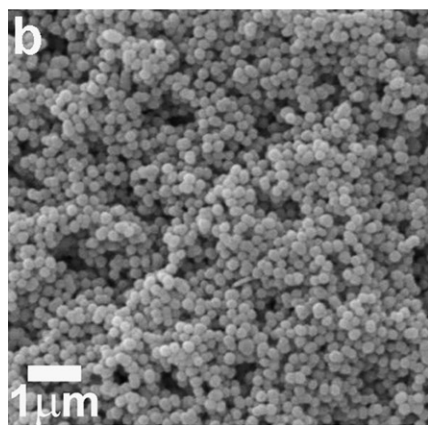
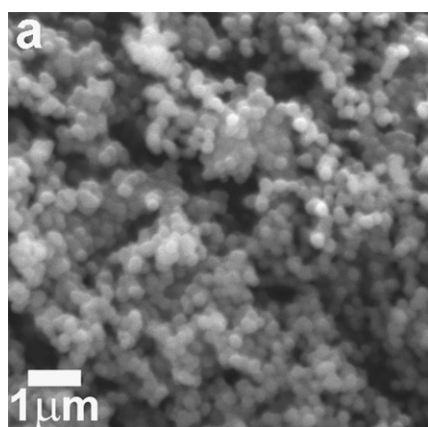


Fig. 2. (a–c) SEM images of the ZnS-140, ZnS-160 and ZnS-180 nanospheres. (d–f) Particle size distributions of the ZnS-140, ZnS-160 and ZnS-180 nanospheres.

aqueous solution (200 ppm). The mixture was stirred in dark for 1 h to establish adsorption/desorption equilibrium. Then the system was exposed to 300 W highly pressure mercury vapor lamp at 365 nm for photocatalysis reaction under moderate stirring. At regular intervals, the suspension was taken from the vessel and centrifuged. The content of RhB in supernatant was determined by UV–Vis spectroscopy at 554 nm. For comparison, the photocatalytic activity of the commercially available TiO_2 (Degussa P25) was also determined.

The formation of $\cdot\text{OH}$ on the photo-irradiated ZnS nanospheres' surface was detected *in situ* by a fluorimetric assay using terephthalic acid (TPA) as a probe under photocatalytic conditions except the replacement of RhB with TPA. The photo-irradiation was employed and the suspension was taken from the reactor. Subsequently, the suspension was centrifuged to detect the fluorescent intensity of 425 nm by excitation with 315 nm irradiation.

3. Results and discussion

From the XRD patterns of the ZnS nanospheres (Fig. 1), all the nanospheres exhibit similar XRD patterns, in which seven peaks at 27.18, 28.64, 30.50, 39.62, 47.75, 52.02 and 56.53 correspond to the (100), (002), (101), (102), (110), (103) and (112) planes of the wurtzite phase (JCPDF 36-1450), respectively. It should be noted that all the diffraction peaks are relatively broad, which can be attributed to the small size of the nanospheres.

From the SEM images (Fig. 2a–c), all the samples present spherical morphology with narrow particle size distributions. The mean diameters of the ZnS-140, ZnS-160 and ZnS-180 nanospheres are 230.3, 169.7 and 233.5 nm, respectively. The ZnS-160 nanospheres are much smaller than the ZnS-140 and ZnS-180 nanospheres. This indicates that the temperature can affect the size of the nanospheres and the size of the nanospheres can be controlled by the temperature. From the BET analysis, the SSA of the ZnS-140, ZnS-160 and ZnS-180 nanospheres are 131.2, 222.4 and 108.0 m²/g, respectively. The SSA of ZnS-160 nanospheres are much higher than those of the ZnS-140 and ZnS-180 nanospheres, which can be attributed to the smaller size of the ZnS-160 nanospheres.

In addition, the reaction time was prolonged to 12 and 24 h at 160 °C to determine the effects of the reaction time on the size of the nanospheres. From the results (Fig. 3a and b), the products obtained after reacted for 12 and 24 h also exhibit the similar spherical morphology to the product of 6 h. However, the mean diameters are 203.1 (12 h) and 268.5 nm (24 h) (Fig. 3c and d), respectively, much bigger than that of the 6 h product. This

suggests that the reaction time can influence the size of the nanospheres and the size of the nanospheres can also be controlled by the reaction time.

From the UV–vis spectra of the ZnS nanospheres (Fig. 4a), all the samples present the broad absorption peaks centered at 339 nm for ZnS-140, 326 nm for ZnS-160 and 340 nm for ZnS-180. The absorption peak of the ZnS-160 nanospheres shows an obvious blue shift compared with those of ZnS-140 and ZnS-180 nanospheres. This can be attributed to the smaller size of the ZnS-160 nanospheres.

Because of the strong photo absorption property, the photocatalytic activities of the ZnS nanospheres to degrade RhB under UV light irradiation were studied. From the results (Fig. 4b), after 120 min irradiation, the photodegradation efficiencies of the ZnS-160 nanospheres is 96.6%, much higher than those of the ZnS-140 (28.8%), ZnS-180 (44.1%) and the P25 (75.7%). The excellent photodegradation performance of the ZnS-160 nanospheres can be attributed to the largest SSA in the three ZnS samples, which can afford the much more active sites accessible for the photodegradation reaction. The degradation spectra of RhB under the treatment of ZnS-160 nanospheres also confirm its good photodegradation performance on RhB (Fig. 4c). Furthermore, the inductively coupled plasma–mass spectrometry (ICP–MS) analysis showed that there was only a trace amount of Zn²⁺ in the supernatant after the photocatalysis, suggesting the stability of the ZnS nanospheres.

From the literature, as one of the key active intermediates, hydroxyl radical ([•]OH) plays the important function in the photocatalytic degradation of organic dyes [14]. Therefore, the [•]OH generated on the photoilluminated ZnS nanospheres' surface

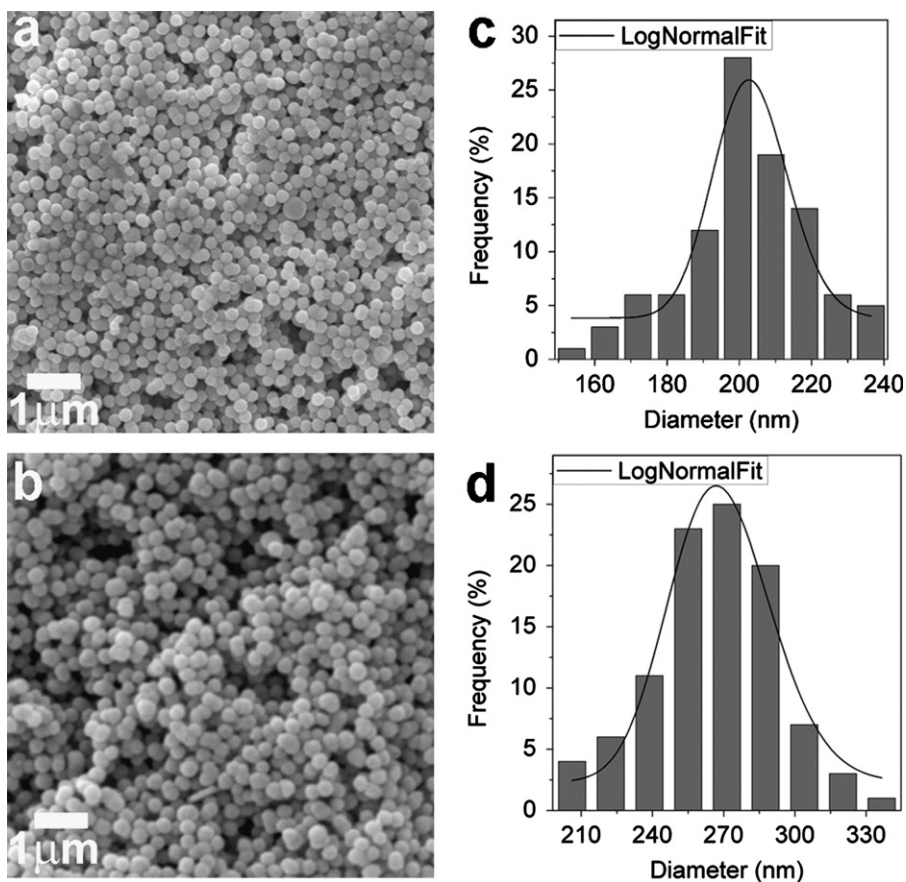


Fig. 3. (a–b) SEM images of the ZnS nanospheres obtained for 12 and 24 h at 160 °C. (c–d) Size distribution analysis of the ZnS nanospheres obtained for 12 and 24 h at 160 °C.

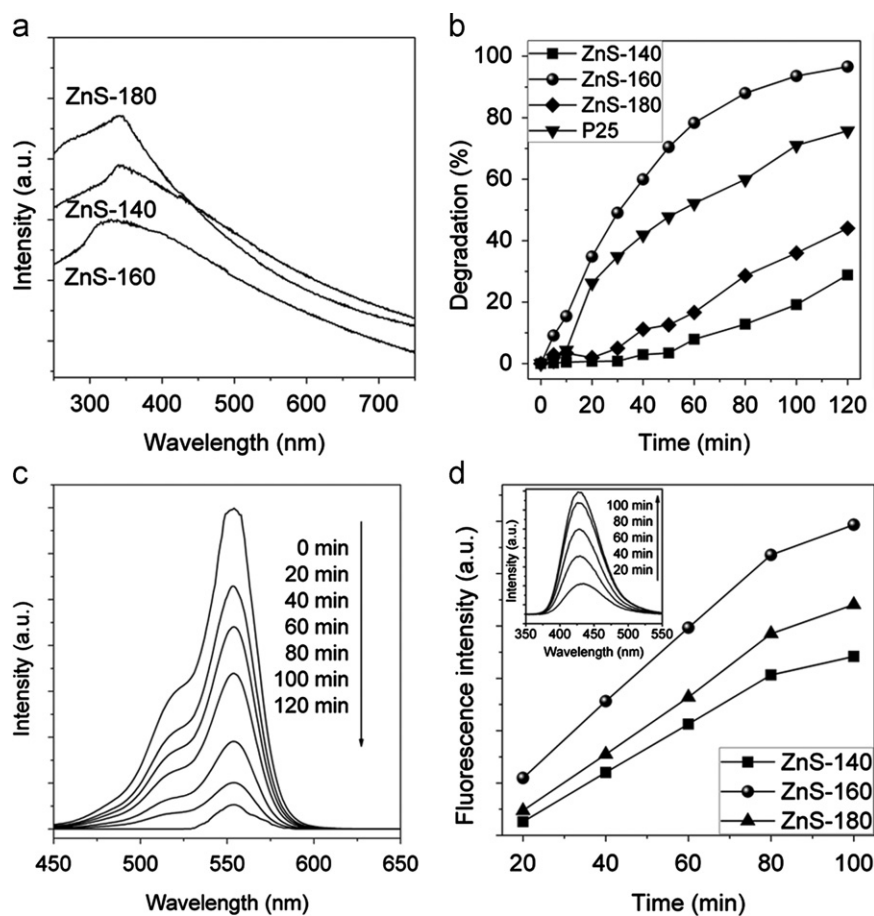
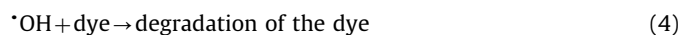


Fig. 4. (a) UV-vis spectra of the ZnS nanospheres. (b) Photocatalytic degradation of RhB in the presence of different samples. (c) UV-vis spectra of RhB after degraded by ZnS-160 nanospheres for different intervals. (d) PL intensity at 426 nm against irradiation time for TPA on ZnS-140, ZnS-160 and ZnS-180 nanospheres. Inset: PL spectra against irradiation time for TPA on ZnS-160 nanospheres.

was detected *in situ* by fluorimetric assay [4,15]. From the results (Fig. 4d), with the irradiation time increased, the photoluminescence (PL) intensities increase gradually, demonstrating the successive generation of $\cdot\text{OH}$. Moreover, the PL intensities of the three nanospheres are different, revealing their different $\cdot\text{OH}$ production efficiencies. The $\cdot\text{OH}$ production efficiency of the ZnS-160 nanospheres is significantly higher than those of the ZnS-140 and ZnS-180 nanospheres, consistent with the photocatalytic activities. Based on these results, the photocatalytic degradation mechanism of RhB in the presence of ZnS nanospheres is proposed. Firstly, the photons owning the energy higher than that of the nanospheres' band gap are firstly absorbed onto the nanospheres' surface. This will excite the electrons from valence band (vb) to conduction band (cb), generating positive hole (h_{vb}^+) at the valence band edge and electron (e_{cb}^-) in the conduction band (Eq. (1)). Secondly, h_{vb}^+ and e_{cb}^- can react with water or hydroxyl groups and generate $\cdot\text{OH}$ (Eqs. (2) and (3)). Finally, $\cdot\text{OH}$ can react with RhB molecules to exert the degradation (Eq. (4)).



4. Conclusions

In summary, well-dispersed ZnS nanospheres were successfully prepared in large scale through a facile hydrothermal approach. Through the mediation of photo-generated $\cdot\text{OH}$, the ZnS nanospheres exhibited strong photocatalytic activities to degrade the organic dyes under UV light irradiation, suggesting the potential application in the efficient treatment of the organic pollutants.

Acknowledgments

This work was financially supported by the National Natural Science Foundation of China (21171051, 21271066, U1204516) and the Program for Changjiang Scholars and Innovative Research Team in University (IRT1061) and the Innovation Fund for Outstanding Scholar of Henan Province (114200510004) and the Key Young Teachers Project of Henan Province (2012GGJS-065) and Henan Normal University.

References

- [1] Mathur N, Bhatnagar P, Nagar P, Bijarnia MK. *Ecotoxicol Environ Saf* 2005;61:105–13.
- [2] Verma AK, Dash RR, Bhunia P. *J Environ Manage* 2012;93:154–68.
- [3] Fan Y, Deng M, Chen G, Zhang Q, Luo Y, Li D, et al. *J Alloys Compd* 2011;509:1477–81.
- [4] Yu X, Yu J, Cheng B, Huang B. *Chem—Eur J* 2009;15:6731–9.
- [5] Asahi R, Morikawa T, Ohwaki T, Aoki K, Taga Y. *Science* 2001;293:269–71.
- [6] Liu M, Piao L, Zhao L, Ju S, Yan Z, He T, et al. *Chem Commun* 2010;46:1664–6.

- [7] Chen D, Huang F, Ren G, Li D, Zheng M, Wang Y, et al. *Nanoscale* 2010;2:2062–4.
- [8] Guo Y, Jiang L, Wang L, Shi X, Fang Q, Yang L, et al. *Mater Lett* 2012;74:26–9.
- [9] Guo Y, Wang J, Tao Z, Dong F, Wang K, Ma X, et al. *CrystEngComm* 2012;14:1185–8.
- [10] Liu Y, Hu J, Zhou T, Che R, Li J. *J Mater Chem* 2011;21:16621–7.
- [11] Muruganandham M, Amutha R, Sillanpää M. *ACS Appl Mater Interfaces* 2010;2:1817–23.
- [12] Zhang Y, Xu H, Wang Q. *Chem Commun* 2010;46:8941–3.
- [13] Zhao Y, Zhang Y, Zhu H, Hadjipanayis GC, Xiao JQ. *J Am Chem Soc* 2004;126:6874–5.
- [14] Ishibashi K-i, Fujishima A, Watanabe T, Hashimoto K. *Electrochem Commun* 2000;2:207–10.
- [15] Zhao W, Sun Y, Castellano FN. *J Am Chem Soc* 2008;130:12566–7.